AAPT PHYSICS EDUCATION | AMERICAN JOURNAL of PHYSICS

Aerodynamics of the knuckleball pitch: Experimental measurements on slowly rotating baseballs

John P. Borg and Michael P. Morrissey

Citation: American Journal of Physics **82**, 921 (2014); doi: 10.1119/1.4885341
View online: http://dx.doi.org/10.1119/1.4885341
View Table of Contents: http://scitation.aip.org/content/aapt/journal/ajp/82/10?ver=pdfcov
Published by the American Association of Physics Teachers

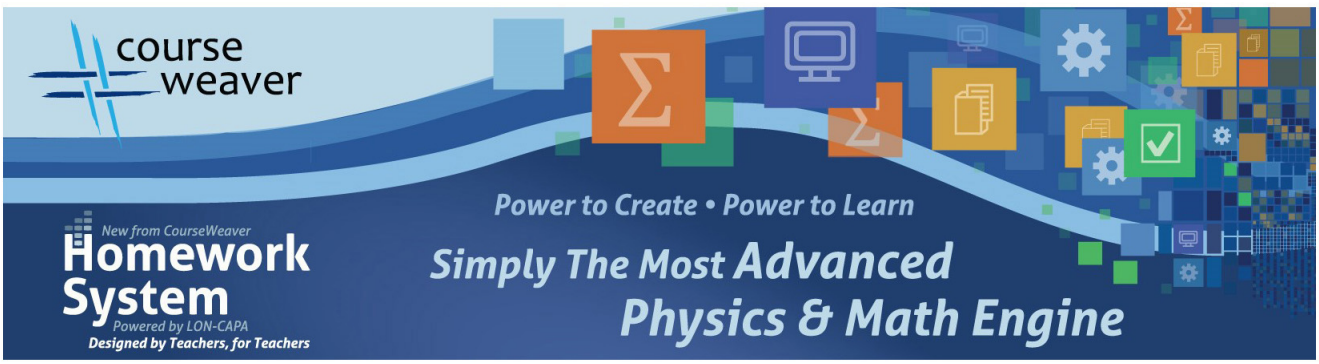

Aerodynamics of the knuckleball pitch: Experimental measurements on slowly rotating baseballs

John P. Borg[a] and Michael P. Morrissey
Department of Mechanical Engineering, Marquette University, 1515 W. Wisconsin Avenue, Milwaukee, Wisconsin 53233

(Received 31 August 2013; accepted 9 June 2014)

In this work, we characterize the lift and lateral forces on a two-seam versus four-seam knuckleball and measure the viscous shear stress. We believe these measurements to be the first reported for slowly rotating baseballs. Our findings indicate the seam acts to either delay or advance separation depending upon the ball angle; these results are supported with flow visualization. The combined effect produces significant lift and lateral forces that can rapidly change as the ball rotates. Furthermore, we found the shear stress to be asymmetric which can result in significant in-flight torque. Together, asymmetries in force and shear stress produce the complicated flight trajectories that can confound the hapless batter. © *2014 American Association of Physics Teachers.*
[http://dx.doi.org/10.1119/1.4885341]

I. INTRODUCTION

A. Knuckleball background

In 1671, Newton observed that a tennis ball's trajectory could be altered as a result of spin.[1] Thus, the aerodynamically induced motion of sports balls has long been a subject of interest to players and physicists alike.[2–19] Pitchers take advantage of these effects with an arsenal of different breaking pitches: sliders and curveballs, sinkers, cutters, and the ever-confounding knuckleball. Each pitch is delivered with aerodynamics in mind, from the way the pitcher grips the ball and aligns the seams, to the initial velocity, spin, and axis of rotation. Rapidly spinning a ball in flight results in a Magnus force that is perpendicular to the axis of rotation and linearly increases with spin rate.[20] Breaking ball pitchers seek to maximize spin rates, which have been measured in game conditions as high as 3000 rpm[10,21] However, the knuckleball varies from all other breaking pitches in a significant way—it is thrown with very little spin. The result is an aerodynamic force that changes direction and magnitude during flight, giving rise to an unpredictable flight trajectory that confuses the batter and catcher alike.

The knuckleball pitch appeared early in the 20th century and is credited to pitcher Eddie "Knuckles" Cicotte.[22] Through trial and error, pitchers have optimized the ball orientation and delivery to take advantage of aerodynamic asymmetries. Two recent Major League Baseball (MLB) pitchers, Dickey and Tim Wakefield, deliver the knuckleball from their fingertips in a velocity range from 22 m/s to 38 m/s (50 to 85 mph) utilizing a two-seam orientation. It is extremely important that the ball rotate forward one half rotation, so that both seams cross stagnation (the location on the front of the ball where the local flow velocity comes to rest).[22,23] At a pitch distance of 18.4 m (60 ft 6 in.) this translates to a rotation rate of approximately 50 rpm, much lower than typical breaking pitches. The resulting pitch is arguably the most difficult to hit in all of baseball. Several videos of Dickey pitching, with analysis and discussion, can be found at Alan Nathan's website.[24] In addition, the interested reader should investigate the feature length documentary film that follows MLB's only knuckleballers in 2011: Dickey and Wakefield.[25]

In baseball terminology, there are two generalized ball orientations: two-seam (2S) and four-seam (4S), both of which are illustrated in Fig. 1. A 2S pitch is one in which only two seams pass through stagnation per ball revolution, whereas a 4S pitch has four seams pass through stagnation per revolution. The cover of a baseball is constructed from two hourglass shaped pieces of cowhide. The rounded ends of the hourglass are referred to as the horseshoe, whereas the long middle section is referred to as the runway or landing strip.

Figure 1(b) illustrates the momentum boundary layer and associated terminology. In this illustration, the boundary layer on top remains laminar until it separates from the ball near $\theta_{s,top} = 110°$, measured counterclockwise (CCW) from stagnation. Whereas the boundary layer on bottom is tripped by the seam and transitions from laminar to turbulent at the critical transition angle θ_c as measured clockwise (CW) from stagnation. The turbulent boundary layer is better able to negotiate the curvature of the ball and the adverse pressure gradient to remain attached to the ball longer but eventually separates near $\theta_{s,bottom} = 120°$ CW. The separation angle on the bottom of the ball is delayed (larger) compared to the separation angle on the top of the ball, which results in a turbulent wake that is shifted upward, i.e., there is an upward momentum displacement.[6,15] The result is a reaction force acting on the ball in a downward (negative lift) direction. Thus, the ball in Fig. 1(b) would experience negative lift.[26] As a general rule, one can expect the ball to have a force on the side of the ball where a seam is closest to stagnation.

B. Aerodynamics background

With a pitch velocity range between 22 m/s to 38 m/s, the Reynolds number $\mathrm{Re} = UD/\nu$ ranges from about 1.0×10^5 to 1.8×10^5. Here U is the ball velocity, D is the ball diameter (74 mm), and ν is the kinematic viscosity of air (15.6×10^{-6} m^2/s). For smooth spheres, this range of Reynolds number is subcritical, which means the boundary layer around the ball should remain laminar up until it separates; the separated wake is always turbulent. As the flight velocity increases, however, the boundary layer can transition from laminar to turbulent at the critical transition Reynolds number near 2×10^5. The turbulent transition initially occurs at a critical angle θ_c near 100° and moves forward, towards stagnation, as the Reynolds number is increased. At Reynolds numbers greater than 10×10^5 the entire boundary layer is turbulent.[27]

These Reynolds number ranges are specific to smooth spheres and are sensitive to surface roughness.[9] Achenbach

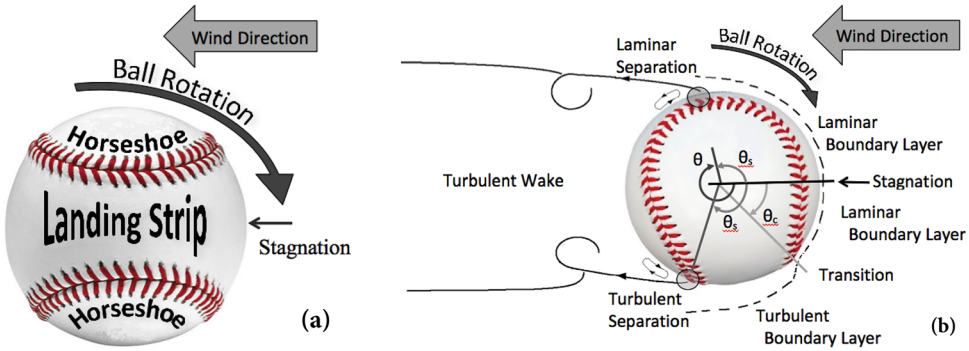

Fig. 1. Baseball and aerodynamic orientation with nomenclature as the ball is pitched from left to right: (a) four-seam (4S) orientation; (b) two-seam (2S) orientation.

measured the separation angle on smooth and rough spheres at the subcritical Reynolds number of 1.6×10^5 and found that it varied from 82° to 100° to 120° for surface roughness ratios of $k/D = 0$, 250×10^{-5}, and 1250×10^{-5}, respectively, where k is the characteristic height of the roughness and D is the diameter of the sphere.[28] In more recent work, roughness ratios (k/D) between 1000×10^{-5} and 4000×10^{-5} on spheres were investigated at Reynolds numbers ranging from 5×10^4 to 5×10^5 and the effects on separation was surprisingly localized.[29] The seam heights of official MLB baseballs have been measured to vary between 0.686 and 0.889 mm.[30] The average seam heights for the balls used in this study were 0.722 mm ($k/D = 975 \times 10^{-5}$) and are therefore sufficiently large to qualify as "roughness" at the Reynolds numbers of interest; they can trip the boundary layer and result in asymmetric aerodynamic loading. The average seam height for a Rawlings official high school baseball (R100HS) is larger, near 1.22 mm, demonstrating that there can be significant differences between baseball types.

In addition to tripping the boundary layer and delaying separation, the seams can directly cause separation. Separation can affix itself to the seam and be either advanced or delayed as the ball is rotated.[7] Such an effect occurs over a narrow window of ball angles when a seam is near the natural separation angle. Thus, the seams have multiple mechanisms by which they influence separation and the aerodynamics: tripping the boundary layer to induce turbulence, thereby delaying separation; or directly forcing separation to occur, thereby advancing/delaying separation. In so doing, complicated aerodynamic forces and flight paths result.

Our objective is to understand what mechanisms generate aerodynamic forces on a knuckleball in order to maximize the effectiveness of the pitch. To accomplish this, we will measure and compare 2S versus 4S lift and lateral force data from baseballs rotating at 50 rpm. Many aerodynamic measurements have been made on baseballs; however, in previous work, the balls are either rapidly spinning or stationary. In addition, we want to measure the fluidic shear stress and characterize the resulting torque while rotating the ball at 50 rpm. To our knowledge, our shear and force measurements are unique in the literature.

II. EXPERIMENTAL SETUP

Experiments were conducted in Marquette University's closed-loop wind tunnel that has a cross-sectional test area of 0.372 m^2 (2 ft × 2 ft). The velocity variation across the test section is less than ±1% of the mean, with a turbulence intensity level of approximately 0.25%. Flow visualization was accomplished utilizing neutrally buoyant helium filled 1.3-mm (1/20-in.) diameter soap bubbles.[31–33] The baseballs used in this study were official Rawlings MLB baseballs in order to insure consistent seam height and ball obliquity (roundness); however, these balls were not treated with rubbing mud, which may affect surface roughness. The dimensions and construction of official MLB baseballs are governed by rule 1.09 in the Official Rules of Baseball, which states that balls shall weigh not less than five nor more than 5 1/4 ounces and measure not less than nine nor more than 9 1/4 in. in circumference.[34] More than 20 different baseballs were used in this study, all of which adhered to these standards. The following introduces the measurements made; the interested reader should see Morrissey for a more complete description.[2]

A. Force measurements

The baseballs were pedestal mounted on a two-axis force balance in order to measure lift (up-down) and lateral (side-to-side) forces. Forces were non-dimensionalized by dividing by the dynamic pressure times the projected ball area

$$C_L = \frac{\text{Force}}{\rho U^2 A_D/2}, \tag{1}$$

where ρ is the air density, U is the free stream velocity, and A_D is the projected ball area. The uncertainty in lift coefficient was calculated to be near 0.001, which is on the order of 0.2% error using the propagation of uncertainty method.[2,35]

The force balance was fit with a motor that could spin the ball at a given rate or rotate the ball to a specified azimuthal angle. An optical chopper plate was used to measure the angular position to within ±0.15°. Data were collected for 300 ball rotations at a sample frequency of 2000 Hz and was repeated 9 times; the resulting data were ensemble averaged. Care was taken to avoid spinning the ball or sampling data near the ball shedding frequency. For a Strouhal number ($\text{St} = fD/U$) of 0.2, the shedding frequency f is approximately 84 Hz for a pitch velocity of 31 m/s (70 mph). The ball rotation frequency was 0.83 Hz (50 rpm), which is noncontiguous with the sample rate and well below the Nyquist frequency.

B. Shear-stress measurements

Shear stress measurements were made on the surface of the baseball using several hot-film anemometers. The

anemometers were constructed in house using 5-μm diameter tungsten wire with an electrical resistivity of 52.8 nΩ·m at 20 °C and calibrated using the Blasius profile and smooth sphere data.[28,36,37] Shear stress measurements τ_w were non-dimensionalized by the dynamic pressure

$$C_s = \frac{\tau_w \sqrt{\mathrm{Re}}}{\rho U^2/2}. \tag{2}$$

The associated error in shear stress was estimated, using a propagation of uncertainty analysis, to be 0.0025 N/m^2, which translates to less than 0.1%.[35]

III. RESULTS

A. Flow visualization

Flow visualization was used to measure the boundary layer separation angles. Flow around a smooth sphere at a Reynolds number of 2×10^5 produces a laminar boundary layer that separates near 82° from stagnation.[28,38] We measured the smooth sphere separation angle to be $81° \pm 5°$, which is in good agreement with the 82° reported by Achenbach. Figure 2 presents two ensemble averaged photographs constructed by superimposing 57 images taken while the baseball was in a 2S orientation at a Reynolds number of 2×10^5. The separation angle varies from 88° to 122° as the ball undergoes one rotation, with an average (107°) that is much larger than the smooth sphere.

Figure 2(a) presents the 2S ball at an angle of 225°. The boundary layer on top remains somewhat laminar, although the seams on the bottom have tripped the boundary layer to turbulent, thereby delaying separation. Separation from both the top and bottom of the ball ($\theta_{s,top} = 107°$, $\theta_{s,bottom} = 118°$) exceeds the laminar separation angle of 81° due to surface roughness and three-dimensional effects. Since the helium bubbles move in or out of the light sheet, streaklines may appear to stop and start, which is an indication of three-dimensional flow structures.[10,13,18] Figure 2(b) presents the ball at an angle of 285°, where the top separates much earlier than the bottom: $\theta_{s,top} = 95°$ and $\theta_{s,bottom} = 117°$, respectively. Video images show the separation locking-onto to the bottom seam and being dragged back with the seam as the ball rotates.[39]

B. Induced rotation

In order to characterize aerodynamically induced ball rotation, the driver motor was removed so that the ball was free to rotate. For Reynolds number below 1.5×10^5, for any given initial angle and rotation rate, a ball in a 4S orientation would rotate and come to rest such that a seam was located at stagnation, presenting a symmetric seam pattern to the wind. For Reynolds numbers above 1.5×10^5, the ball is sensitive to the initial rotation rate. If the ball is initially rotating at 50 rpm, it will spin up to a rotation rate near 100 rpm. The spin rate increases linearly with Reynolds number, becoming constant at 180 rpm for all Reynolds numbers greater than 2×10^5, when rotation is limited by the net shear stress and the inertia of the ball.

A ball in a 2S orientation, for any initial angle or rotation rate, would eventually rotate to an angle of either 90° or 270° at which point it would oscillate at 1 Hz with a peak-to-peak amplitude of 45°. The oscillation frequency was constant over a Reynolds number range from 1.9×10^5 to 4.6×10^5. Coincidentally, a 2S ball at angles of 90° or 270° present the same seam pattern to the wind as a 4S ball at angles of 0° or 180°; only the lift and lateral directions are reversed. Therefore, it would be difficult to throw a pitch that did not begin to rotate under the influence of aerodynamic shear. Given the short time of flight however, significant rotation may not be realized.

C. Force measurements: Four-seam (4S) orientation

Lift and lateral force measurements were collected on spinning and non-spinning baseballs. Figure 3 presents the averaged dimensionless lift from a non-spinning ball in a 4S orientation as a function of ball angle at a Reynolds number of 1.6×10^5. The data of Watts and Sawyer[7] and Higuchi and Kiura[19] are presented for comparison. Pictures illustrating the seam locations for corresponding ball angles are displayed directly below the x-axis for reference. The Marquette data compare favorably to the Watts and Sawyer data, but Higuchi and Kiura report much larger lift coefficients. Higuchi and Kirura used a Rawling OLB3 baseball, which has significantly higher seam heights as compared to a MLB baseball; the higher seam could explain the higher lift data. The four period waveforms of all three data sets are the same; each passes through zero when a symmetric seam pattern is presented to the wind. In general, the force is towards the side of the ball in which a seam is closest to stagnation. The lateral force, not presented, is near zero for all ball angles because the ball presents a symmetric seam pattern to the wind; only asymmetries result in net forces. Finally, it is worth repeating that this lift force is not a Magnus force but instead the result of seams delaying or advancing separation,

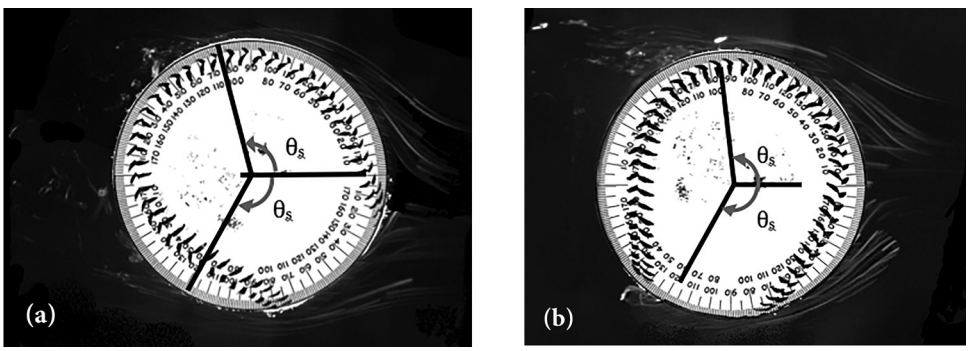

Fig. 2. Superimposed flow visualization images used to measure separation angle in two-seam orientation: (a) ball angle $\theta = 225°$, separation angles $\theta_{s,top} = 107°$ and $\theta_{s,bottom} = 118°$; (b) ball angle $\theta = 285°$, separation angles $\theta_{s,top} = 95°$ and $\theta_{s,bottom} = 117°$.

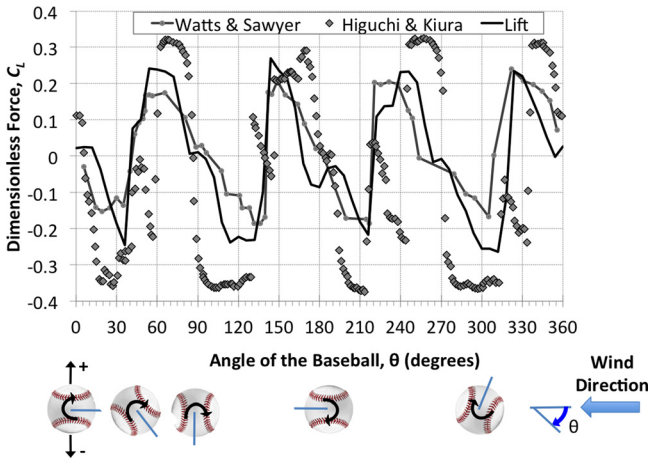

Fig. 3. Dimensionless lift data for a non-spinning ball in a 4S orientation.

bending the wake either up or down, as described in the introduction.

Figure 4 presents lift data from spinning (50 rpm) and non-spinning 4S balls. The spinning-ball data exhibit the same periodicity as the non-spinning data; however, the average lift force per ball revolution is near $C_L = 0.03$, resulting in a slight positive lift force bias compared to the non-spinning ball. This bias results from separation being dragged towards stagnation on the topside of the ball and being pulled away from stagnation on the bottom side of the ball. The effect enhances the pressure recovery on the bottom as compared to the top, which results in an upward bias.

Although Figs. 3 and 4 present averaged data, there were significant fluctuations in lift. The standard deviation, used to characterize the fluctuations, varied between 0.07 and 0.17 for one ball revolution, which is significant considering the maximum lift coefficient is near 0.25. The largest fluctuations occur as the ball passes through symmetry and the lift changes sign.[7] The standard deviation in lift increases for a spinning ball to just over 0.2 and is nearly constant as a function of ball angle. This could be related to the seams continuously disrupting the vortex shedding as the ball rotates. These results complicate the aerodynamics of slowly spinning knuckleball pitches.

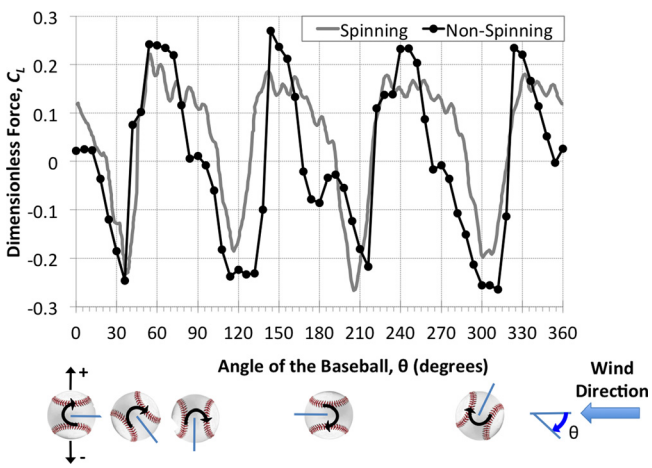

Fig. 4. Dimensionless lift coefficient for a spinning (50 rpm) and non-spinning ball in a 4S orientation.

D. Force measurements: Two-seam (2S) orientation

Figure 5 presents the lateral and lift force for a non-spinning baseball in a 2S orientation obtained at a Reynolds number of 1.6×10^5. Included on this figure are data obtained from Higuchi and Kiura[19] and a pitch window, illustrated as a shaded region from 120° to 300°, which represents the desired ball rotation of Dickey and Wakefield.[22,23] The lift and lateral force data for the 2S pitch contain much more structure compared to the 4S pitch. In a 4S orientation, there is always a seam between stagnation and separation on both sides of the ball, which may aid smoothing the waveforms observed in Figs. 3 and 4. However, in a 2S orientation, there are ball angles for which there can be seams only on one side of the ball, which creates more asymmetry.

Given this asymmetry, the lift forces are anti-symmetric about 180°—the lift forces from 180° to near 360° have the opposite sign of the lift forces from 180° to near 0°. The local force maxima (positive or negative) correspond to angles where the seams affect both the boundary layer and separation. It is no surprise that the pitch window corresponds to ball angles where the seam rotates through stagnation thereby reversing the force direction. This situation would create a large aerodynamically induced change in forces during the pitch. Much like the 4S orientation, the lateral force measured for the 2S orientation is relatively small compared to the lift forces.

Figure 6 compares the lift coefficient from spinning and non-spinning baseballs in a 2S orientation. The spinning lift exhibits the same periodicity as the non-spinning lift with a slight shift in phase and an average lift coefficient per revolution slightly above zero, as was observed and discussed for the 4S ball. The standard deviation in the 2S non-spinning lift data varies between 0.1 and 0.5, which is significant given the maximum lift coefficient is near 0.25. For the spinning 2S ball, the standard deviation in the lift coefficient is just over 0.5 and is nearly constant as the ball rotates through one revolution. Thus, there are significant occurrences where the lift changes sign. Although the average 2S lift is comparable to the 4S lift, the variation in force for the 2S knuckleball is much larger than the 4S knuckleball.

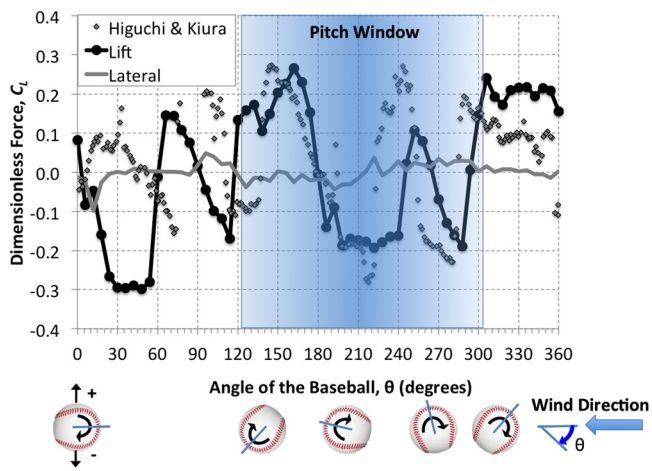

Fig. 5. Comparison of lateral and lift coefficient for a non-spinning ball in a 2S orientation at a Reynolds number of 1.6×10^5. Current data are compared with data from Higuchi and Kiura.

E. Shear stress measurements

Hot-film anemometry was used to measure the viscous shear stress at the center of the landing strip in a 2S orientation as a function of ball angle. Measurements were also made on a smooth sphere that could be fit with a 1.3-mm tall tripwire placed 60° from the hot-film. Figure 7 presents the ensemble averaged data collected for 30 ball rotations while spinning at 50 rpm at a subcritical Reynolds number of 1.6×10^5; smooth sphere data have been included for comparison.[27] A pictorial representation of the ball's orientation, where an arrow depicts the location of the hot-film, is also included.

Figure 7 indicates that the shear stress increases as the hot-film is rotated away from stagnation and is exposed to higher wind velocities. The shear stress decreases past 60° as the flow experiences the adverse pressure gradient and begins to slow towards separation. The shear stress on the smooth sphere rapidly approaches zero (i.e., separation) at a ball angle near 85°. Achenbach used a strain gauge arrangement to directly measure fluidic force and was therefore able to distinguish changes in direction of the shear stress. Thus, Achenbach's data change sign as the strain gauge passes through separation and into the recirculating near wake. A single wire hot-film can only measure shear amplitude not direction and therefore remains slightly above zero after separation. In either case, the separation angle for the smooth sphere is near 85°, which is in good agreement with 81° obtained from the flow visualization technique presented above.

The shear stress measured on the smooth sphere with the tripwire follows smooth sphere data until the tripwire crosses stagnation at a ball angle of 60°. At this point, the boundary layer in front of the hot-film is tripped to turbulent, which increases the local shear stress. This effect can clearly be seen as an increase in shear stress near 60°. Subsequent separation does not occur at 85°, as it did for the smooth sphere, but closer to 120° as a result of the turbulent boundary layer.

The shear stress on the baseball has several distinct features as compared to the smooth sphere. For ball angles greater than 35°, the baseball's shear stress is larger than the smooth sphere's shear stress, even with the tripwire. Second, separation from the baseball occurs at 110°, which is much later than the smooth sphere's 85°, but not as late as the 120°

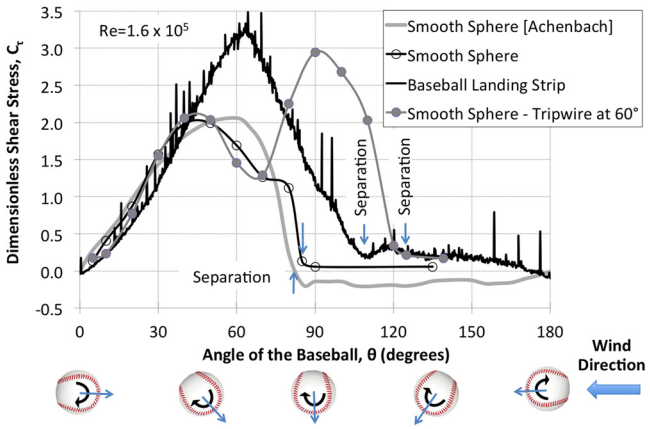

Fig. 7. Shear stress measurements on different spheres as a function of ball angle at a Reynolds number of 1.6×10^5. Vertical arrows represent separation. The arrow on baseball represents hot-film location.

observed for the smooth sphere with tripwire. Thus, although the Reynolds number is subcritical at 1.6×10^5, these observations point to a boundary layer that has transitioned, most likely due to a three-dimensional flow-field. Finally, the separation angle of 110° measured using the hot-film is in good agreement with the flow visualization measurement of 107°.

Figure 8 presents the ensemble averaged shear stress measurements from a hot-film placed 20° from the horseshoe seam, while the baseball rotates either clockwise or counterclockwise at 50 rpm. Thus, the effect of the seam on the shear stress as compared to wind direction—racing into the wind or running with the wind—fore and aft the seam can be assessed. Also included on this figure are measurements obtained from a smooth sphere at two different Reynolds numbers: 1.6×10^5 (subcritical) and 10×10^5 (trans-critical).[27] Since the hot-film passes through stagnation at a ball angle of 135°, the data have been folded back and plotted using two x-axes in order to compare the difference in shear stress as the ball rotates towards and away from stagnation. The arrows in the figure indicate which traces belong to which x-axis. Again, pictorials of the ball have been included for clarity, where the arrow represents the location of the hot-film.

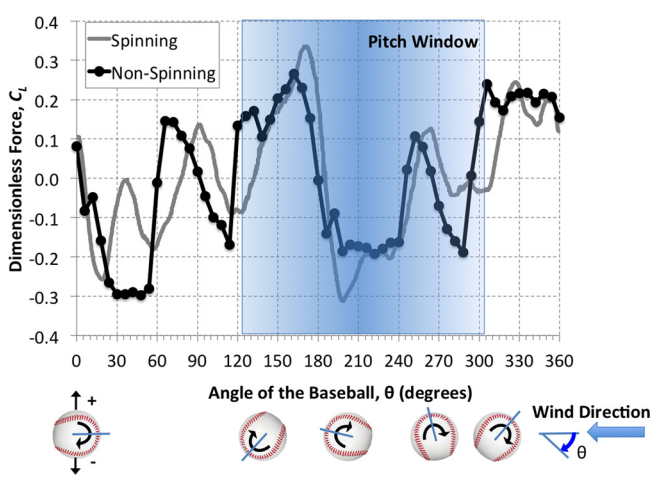

Fig. 6. Comparison of dimensionless lift coefficient for a spinning (50 rpm) and non-spinning ball in a 2S orientation.

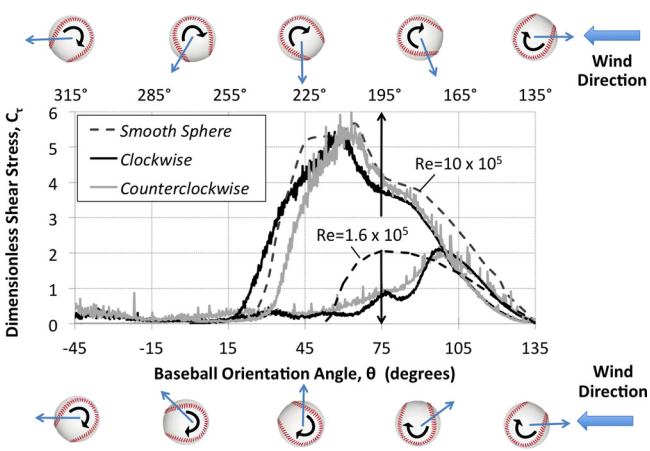

Fig. 8. Shear stress measurements 20° from horseshoe seam while baseball rotated 50 rpm either clockwise or counterclockwise. The arrow on baseball represents hot-film location.

The measurements indicate the dramatic effect the seam has on the local shear stress. When the hot-film is upstream of the seam as the ball rotates from −45° to 135°, the shear stress is smaller than that measured when the hot-film is located behind the seam for the same relative angles. The shear stress in front of the seam is smaller than at the landing strip for the same ball angle (see Fig. 7). Computational Fluid Dynamics (CFD) simulations on a baseball indicate that recirculation occurs near the seams.[40] Thus, the reduced shear could be due to a local slowing or recirculation upstream of the seam. The shear stress downstream of the seam from 135° to 315° is nearly twice that in Fig. 7 at the landing strip for the same relative ball angles. This difference in shear stress is due to the fact that the tripwire is 60° upstream of the hot-film on the smooth sphere (Fig. 7), whereas the seam is only 20° upstream of the hot-film on the baseball (Fig. 8).

The boundary layer separation for clockwise and counterclockwise rotating balls differs. When the hot-film is upstream of the seam, separation occurs near a ball angle of $\theta = 62°$ or separation angle $\theta_s = 73°$ as measured from stagnation (135°–62°). When the hot-film is downstream of the seam, separation occurs near $\theta_s = 111°$ (135°–24°). There is also a difference in separation of nearly 8° depending on if the ball is racing into the wind or running with the wind. These measurements are in agreement with the flow visualization and bias in force measurements presented earlier; both are a direct result of spin.

F. Shear stress integration: Applied torque

Because pressure acts normal to the ball's surface, pressure asymmetries cannot result in ball torque; only asymmetric viscous shear stress can produce torque. Asymmetric seam orientations result in asymmetric shear stress on the ball. The shear stress presented in Fig. 8 can be integrated over a rotation to estimate the aerodynamically induced torque. The result is a net counterclockwise torque τ of 3.92×10^{-3} N m. If we assume the ball has no initial spin and has a flight time t of 0.4 seconds, this shear stress would induce a spin of $\omega = (\tau/I)t = 46$ rpm, where $I = mD^2/10$ is the baseball's moment of inertia, with m the baseball's mass and D its diameter. This rotation rate is near the measured rate of 100 rpm discussed earlier. Thus, shear stress is sufficient to induce significant ball rotation in flight. It is interesting to note that the net shear stress for a 2S pitch with initial clockwise rotation acts to rotate the ball counterclockwise. This effect adds to the complexity of the pitch since shear stress can change the rotation direction during flight and is a testament as to the difficulty of throwing a pitch with no rotation.

IV. CONCLUSIONS

Unraveling the aerodynamic mysteries behind a knuckleball is a challenge. Understanding the complex interactions between the ball's seam and the boundary layer is the key to understanding the asymmetries of aerodynamic forces. The seams influence the pitch in two ways: (1) tripping the boundary layer to induce turbulence thereby delaying separation and (2) directly forcing separation to occur off the seam, thereby advancing or delaying separation as the ball rotates.

The lift and lateral forces are more easily understood in light of this phenomenon. The lift force in a 4S orientation is much more regular, owing to the more regular seam pattern presented to the wind. In contrast, the 2S orientation results in more seam asymmetry, which results in more asymmetry in the lift force. In addition, the 2S orientation generates slightly larger maximum lift with a larger standard deviation as compared to the 4S orientation.

A turbulent boundary layer induces higher shear stress compared to a laminar boundary layer. Since the seam affects the laminar-turbulent transition, there can be large asymmetries in shear stress as a function of ball angle. The integrated shear stress produces a net torque that can cause the ball to rotate. Thus, the asymmetric shear stress can act to *destabilize* the pitch by either increasing or decreasing the rotation rate, or even initiating rotation about a different axis, depending on the orientation of the seams during flight.

In our conversation with Dickey, he stated that the 2S knuckleball generates more motion than the 4S. He throws a hard 2S knuckleball up to 82 mph, ideally rotating the ball from 120° to 300° CW in flight. He stated that ideally his pitches will break hard and quick, down and to his left. His observations are partially supported by data presented here. The lift force is positive for ball angles 120° to 180° and then changes sign, while the lateral force is fairly small. With a positive lift force, the hitter would see a pitch that appears to float towards home plate, dropping more slowly than one would expect because the ball actually has lift. The lift force then changes sign and the ball would appear to quickly move down relative to the pre-break trajectory. In baseball terms this is called "falling off the table." This explains the break down but not to the left. More needs to be known about the initial conditions placed on the ball to better understand the break to the left.

The complex interactions arising from the presence of the seam result in asymmetries in the separation, the force distribution, and shear stress around the baseball. The result is an effective erratic flight trajectory that can confound a hapless batter.

ACKNOWLEDGMENTS

The authors would like to thank Notre Dame Professors Robert Nelson and Scott Morris for providing help in getting this project underway. Our thanks to University of Illinois Professor Alan Nathan for sharing his data and illuminating discussions. The authors would also like to thank Raymond Hamilton and Dave Gibas for the hundreds of hours of machining time put into this project. Last, but not least, we would like to thank R. A. Dickey for talking to us about the art and science of the knuckleball pitch.

[a]Author to whom correspondence should be addressed. Electronic mail: john.borg@mu.edu. Tel.: 414.288.7519

[1]Isaac Newton, "A letter of Isaac newton containing his new theory about light and color," Philos. Trans. R. Soc. **6**, 3075–3087 (1671).
[2]Michael P. Morrissey, "The aerodynamics of the knuckleball pitch: An experimental investigation into the effects that the seam and slow rotation have on a baseball," Master's thesis, Marquette University, USA, 2010, <http://epublications.marquette.edu/cgi/viewcontent.cgi?article=1007&context=theses_open>.
[3]C. Frohlich, "Resource Letter PS-2: Physics of Sports," Am. J. Phys. **79**, 565–574 (2011).
[4]R. K. Adair, *Physics of Baseball*, 3rd ed. (Addison-Wesley, New York, 2002).
[5]L. J. Briggs, "Effect of spin and speed on the lateral deflection (Curve) of a baseball; and the magnus effect of smooth spheres," Am. J. Phys. **27**, 589–596 (1959).

[6]F. N. M. Brown, *See the Wind Blow* (Department of Aerospace and Mechanical Engineering, University of Notre Dame, 1971).
[7]R. G. Watts and E. Sawyer, "Aerodynamics of a Knuckleball," Am. J. Phys. **43**, 960–963 (1975).
[8]P. W. Bearman and J. K. Harvey, Aeronaut, Q. **27**, 112 (1976).
[9]Rabindra D. Mehta, "Aerodynamics of sports balls," Annu. Rev. Fluid Mech. **17**, 151–189 (1985).
[10]T. Mizota, H. Kuba, and A. Okajima, "Erratic behaviour of knuckleball," J. Wind Eng. **62**, 3–13 (1995).
[11]Robert G. Watts and Ricardo Ferrer, "The lateral force on a spinning sphere; Aerodynamics of a curveball," Am. J. Phys. **55**, 40–44 (1987).
[12]Rabindra D. Mehta and Jani Macari Pallis, "Sports ball aerodynamics: Effects of velocity, spin, and surface roughness," Mater. Sci. Sports 185–197 (2001).
[13]Taketo MIZOTA and Yoshiyuki KAWAMURA, "3D-Trajectory Analysis of Side-Spin Knuckle Ball and Quasi-Steady Side-Force in Flight," Transactions of the Japan Society of Mechanical Engineers Series B **73**(734), 1981–1986 (2007).
[14]Leroy W. Alaways and Mont Hubbard, "Experimental determination of baseball spin and lift," J. Sports Sci. **19**, 349–358 (2001).
[15]K. Aoki, J. Nagase, and Y. Nakayama, "Dependence of aerodynamic characteristics and flow pattern on surface structure of a baseball," J. Visual. **6**, 185–193 (2003).
[16]Christian Theobalt, Irene Albrecht, Jorg Haber, Marcus Magnor, and Hans-Peter Seidel, "Pitching a baseball—tracking high-speed motion with multi-exposure images," ACM Trans. Graph. **23**(3), 540–547 (2004).
[17]Alan N. Nathan, "The effect of spin on the flight of a baseball," Am. J. Phys. **76**, 119–124 (2008).
[18]K. Aoki, J. Nagase, and Y. Nakayama, "flying characteristics of the new official rubber baseball," J. Visual. **12**, 4 (2009)
[19]Hiroshi Higuchi and Toshiro Kiura, J. Fluids Struct. **32**, 65–77 (2012).
[20]G. Magnus, "On the deviation of projectiles, and: Over a striking appearance with rotating bodies," Ann. Phys. (N.Y.) **164**, 1–29 (1853).
[21]Tom Verducci, "How a Danish tech company is revolutionizing pitching data," si.com, <http://sportsillustrated.cnn.com/2011/writers/tom_verducci/04/12/fastballs.trackman/>, April 12 (2011).
[22]D. Clark, *The Knucklebook*, edited by Ivan R. Dee (Chicago, 2006).
[23]R. A. Dickey, private communication (24 October 2007).
[24]Alan M. Nathan, The Physics of Baseball Web Site, < http://baseball.physics.illinois.edu/knuckleball.html/>.
[25]R. Stern and A. Sundberg, *Knuckleball!*, a documentary film by Major League Baseball Productions (2012).
[26]A. K. Norman, E. C. Kerrigan, and B. J. McKeon, "The effect of small-amplitude time-dependent changes to the surface morphology of a sphere," J. Fluid Mech. **675**, 268–296 (2011).
[27]Elmar Achenbach, "Experiments on the flow past spheres at very high Reynolds numbers," J. Fluid Mech. **54**(3), 565–575 (1972).
[28]Elmar Achenbach, "The effects of surface roughness and tunnel blockage on the flow past spheres," Fluid Mech. **65**(1), 113–125 (1974).
[29]A. K. Norman and B. J. McKeon, "The effect of a small isolated roughness element on the forces on a sphere in uniform flow," Exp. Fluids **51**, 1031–1045 (2011).
[30]L P. Fallon and J. A. Sherwood, *Performance Comparison of the 1999 and 2000 Major League Baseballs* (University of Massachusetts Lowell Baseball Research Center Report, 2000).
[31]T. J. Mueller, "Flow Visulalization by Direct Injection," in *Fluid Mechanics Measurements*, 2 ed. edited by R. Goldstein (1996).
[32]M. Kerho, M. Bragg, and J. Shin, "Helium bubble flow visualization of the spanwise separation on a NACA 0012 with simulated glaze ice," NASA-TM-105742 (1992).
[33]M. Machacek and T. Rosgen, "Development of a Quantitative Flow Visualization Tool for Applications in Industrial Wind Tunnels," in *Instrumentation in Aerospace Simulation Facilities* (19th International Congress ICIASF, Taylor and Francis, 2001).
[34]"Major League Baseball, Official Rules: Objectives of the game," *Major League Baseball*, 6 (2013); available at http://ntrs.nasa.gov/search.jsp?R=20050028493.
[35]S. J. Kline, "The purpose of uncertainty analysis," ASME J. Fluids Eng. **107**, 153–160 (1985).
[36]H. Blasius, "The boundary layers in fluids with little friction," NACA TM **1256**, 2–57 (1950).
[37]J. F. Foss, "Hot Wire Anemometry Probe Fabrication Manual," in *Hot Wire Anemometry Probe Fabrication Manual*, Turbulent Shear Flow Laboratory (Michigan State University) (private communication).
[38]Paul K. Chang, *Separation of Flow*, 1st ed. (Pergamon Press, Oxford, New York, 1970), Vol. 3.
[39]M. Morrissey, YouTube video entitled 2SeamSpinningMovieTracer ModProtractor, <http://www.youtube.com/watch?v=ahdl7N9WsBs>.
[40]R. Himeno, "Computational Study of Influences of a Seam Line of a Baseball on Flows" in *New Developments in Computational Fluid Dynamics* (RIKEN, The Institute of the Physical and Chemical Research, 2005).